Unveiling Organocatalysts Action – Investigating Immobilized Catalysts at Steady-State Operation via Lab-on-a-Chip Technology

Hannes Westphal+,[a] Rico Warias+,[a] Holger Becker,[b] Matthias Spanka,[c] Daniele Ragno,[d] Roger Gläser,[b] Christoph Schneider,[c] Alessandro Massi,[d] and Detlev Belder*[a]

This paper reports a new method for studying stereoselective catalyzed reactions at a small scale. For this purpose, a micro-sized chemical reactor and a chiral chromatographic column were integrated on a single microfluidic chip hyphenated to mass spectrometry. By running the integrated reactor in truly continuous-flow operation with an automated injection strategy, catalytic processes and their stereoselectivity can be observed over an extended range of time with significantly small consumption of samples, solvents, and catalytic material.

Introduction

Flow chemistry and microreactor technologies have emerged as promising tools in modern organic synthesis.[1–4] They impress with a variety of advantages over their batch counterparts.[5–9] Due to more precise control of reaction parameters, such as mixing and residence time, as well as their improved heat and mass transfer, applications of both techniques could help chemists to perform more effective synthesis and also explore new chemical process windows and reaction paths.[10–14] With reduced waste, safer operation, and superior reaction control, processes also show high potential for system integration.[15–21]

Microreactors are not only increasingly used in the production of fine chemicals and active pharmaceutical ingre-dients (APIs);[22–27] they are also utilized by the pharmaceutical and chemical industries for high-throughput reaction screening and optimization.[28–31] These optimized processes can then be scaled-out or scaled-up and adapted to production in subsequent stages. This process is further empowered by the possibilities of in-line or on-line process monitoring and real-time process control, enabling deeper insights ever into chemical transformations.[32–34] A variety of publications exist using spectroscopic methods,[35–42] mass spectrometry,[43,44] and chromatographic methods[45–47] to gain direct analytical feedback. Such insights are of particular importance in the field of catalysis. Despite the enormous advantages, like the acceleration of chemical reactions and access to new chemical structures, catalytic reactions are often of complex nature, and some of their mechanistic relationships are still not fully understood.[48] Particularly for catalytic transformations with challenging stereochemistry, analyses are required, allowing complete structural elucidation and identification. Especially in the pharmaceutical industry, substances are often produced that have to be enantio-pure. Thus, analytical methods that provide information on enantioselectivity are essential for the optimization processes of synthetic pathways.

This requirement also applies to the use of asymmetric organocatalysis, which presents an efficient alternative to enzyme- and metal-catalyzed reactions.[49] Yet, the potential applications of organocatalyzed reactions are still in their infancy, and a more intensified optimization would open up avenues for industrial processes.[50,11]

In order to evaluate catalytic methods, our group has already used Lab-on-a-Chip devices (LOCs) to couple miniaturized chiral high-performance liquid chromatography (HPLC) with synthesis in microflow in a direct manner.[51,52] Since the direct integration of microfluidic valves still represents one major challenge,[34] external hydraulic valve switching was used to direct the fluidic paths. This allowed, for example, efficient transfers of miniature amounts of reactor effluent and thus an analysis of organocatalytic transformations. For example, a seamlessly combined device was used to characterize hetero-

[a] H. Westphal,+ R. Warias,+ Prof. D. Belder
     Institute of Analytical Chemistry
     Leipzig University
     Linnéstraße 3
     04103 Leipzig (Germany)
     E-mail: belder@uni-leipzig.de
[b] H. Becker, R. Gläser
     Institute of Chemical Technology
     Leipzig University
     Linnéstraße 3
     04103 Leipzig (Germany)
[c] M. Spanka, C. Schneider
     Institute of Organic Chemistry
     Leipzig University
     Johannisallee 28
     04103 Leipzig (Germany)
[d] D. Ragno, A. Massi
     Department of Chemical
     Pharmaceutical and Agricultural Sciences
     University of Ferrara
     Luigi Borsari 46
     44121 Ferrara (Italy)

[+] These authors contributed equally to this manuscript.

     Supporting information for this article is available on the WWW under
     https://doi.org/10.1002/cctc.202101148

genized catalysts,[53] which, due to their higher atom efficiency and ease of separation from the reaction mixture, play a much more important role in flow processes. Thus, it was possible to investigate the influence of substrate choice and residence time on product formation and determine enantioselectivity by chip-HPLC/MS.

However, since the external valve control applied so far entailed reactor operation with stopped-flow, a continuous reactor operation could not be studied (schematic in Figure 1A, left). As productive catalytic cycles often compete with side reactions and catalyst deactivation, e.g. decomposition can occur, it is essential to study the operation of such catalytic processes in its steady-state and over an extended time on stream.[50,54,55]

With this work, we present a single chip-device capable of performing heterogeneous catalyzed transformations in truly continuous flow operation while sampling small portions of reactor effluent and analyzing these by chiral HPLC/MS with an automized sampling protocol. In our previous contribution, the integrated reactor was operated in a stopped-flow manner to extend the reaction time.[53] Nevertheless, for a facilitated transfer of results to upscaled methods, a continuous operation is preferred.

With novel integrated design and operation mode of the LOC-device presented here (schematic in Figure 1A, right), we expect to identify leading performance indicators of exemplarily used organocatalysts immobilized on silica as support. Not only the activity and stereoselectivity of the respective catalysts should be analyzed, but also statements about their lifetime can be made.

Results and Discussion

Visualization of the injection principle

The injection principle is based on sampling a small amount directly from the reactor effluent during continuous operation. A general illustration of the injection principle is shown in Figure 2A, and a detailed description and a video can be found in the SI.

For a first investigation of the functionality of the injection principle and thus the setups operation characteristics, Coumarin-120 was injected in the reactor to visualize the flow during the elution and injection mode by observing its fluorescence (as shown in Figure 2B). For this purpose, the chip was placed on an inverted epi-fluorescence microscope connected to a mercury vapor lamp and bandpass filter (350/50 nm) for excitation. The fluorescence signal was then guided through a
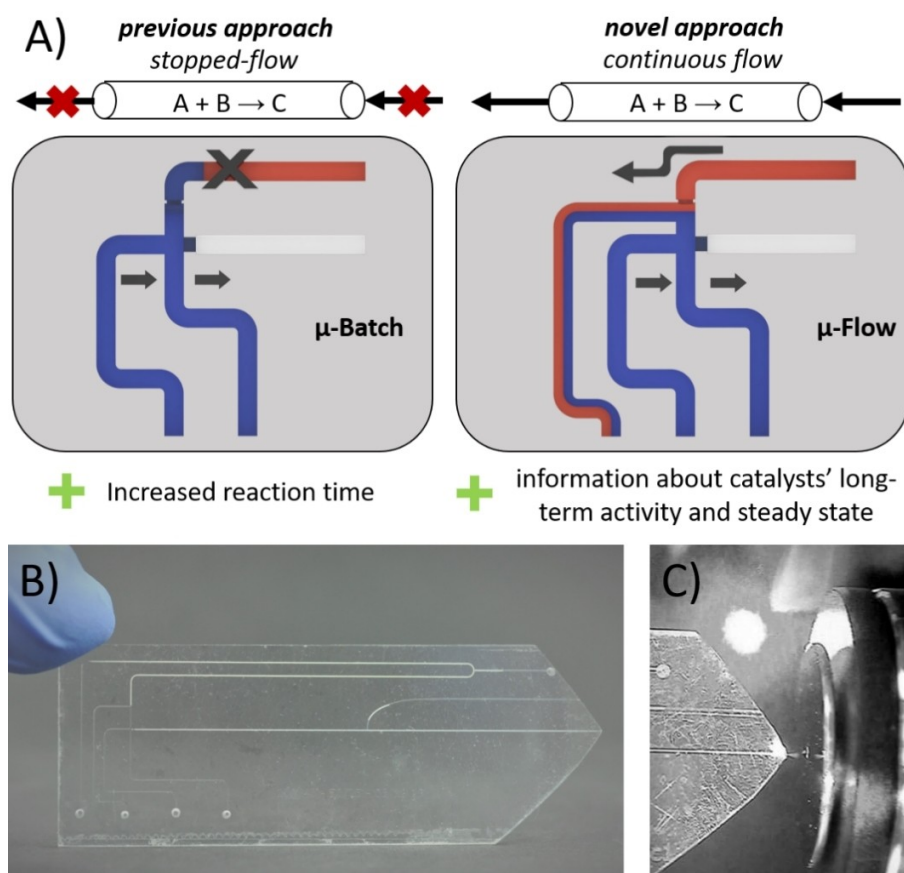

Figure 1. A) Comparison of the newly presented method using a continuous-flow system with our previous approach based on a stopped-flow approach as µ-batch. B) One of the herein presented microfluidic chips with integrated packed bed reactor and chiral chromatographic column. C) Grinded monolithic electrospray emitter.
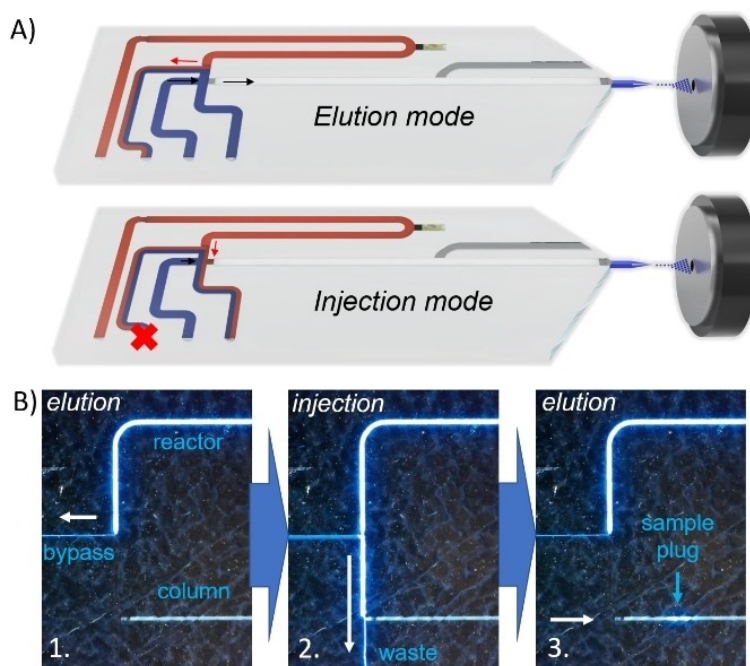
ChemCatChem

Full Papers
doi.org/10.1002/cctc.202101148

Chemistry
Europe
European Chemical
Societies Publishing

Figure 2. Injection principle of the continuous μ-flow reactor on the integrated separation column. Mobile phase 75 μL min^{-1}, H$_2$O:MeCN (55:45 vol.%) with 0.1% FA, 57 bar at injection cross. Pinch flow: 2 μL min^{-1}, H$_2$O:MeCN (50:50 vol.%) with 0.1% FA. Reactor flow: 0.8 μL min^{-1}, 100 μg mL^{-1} fluoranthene in MeCN.

long-pass filter ($>$390 nm) and a dichroic filter (380 nm) before recording using a digital camera.
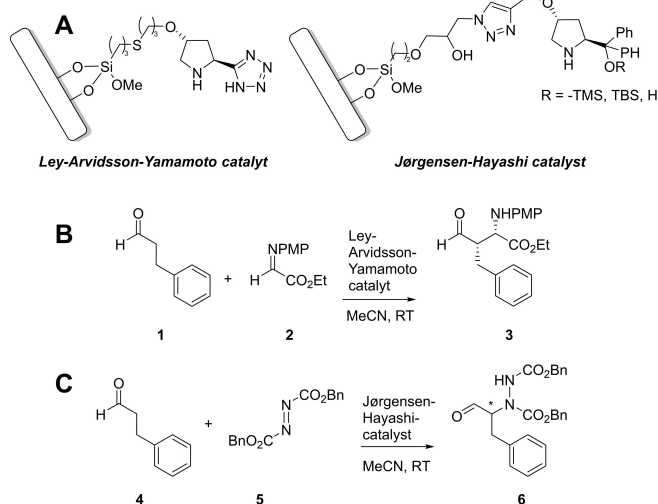
It is shown that during the elution mode (Figure 2B1), the effluent from the reactor outlet continuously flows in the bypass channel, which was connected to the joint restriction and finally to the outlet. The injection cross is kept free of sample solution (here, fluorescent dye) by the elution flow. When switching into injection mode of the reactor, only the bypass channel is blocked, redirecting the reactor effluent stream towards the injection cross and subsequently to a waste channel. During this process, a small portion of the reactor effluent accumulates at the HPLC column head and can then be injected and eluted by switching back into elution mode (Figure 2B3). By varying the injection mode's duration, it was possible to alter the amount of sample injected onto the column head. The injection principle proved to be stable over a reactor flow rate range of 0.1–1.0 μL min^{-1} and an eluent flow rate of 75–125 μl min^{-1}. Additionally, it was possible to use multiple solvents for the sample stream through the reactor (including MeOH, EtOH, MeCN, and DCM) depending on the overall pressure and mixing behavior with the eluent. Generally, to maintain the stability of the injection principle and the continuous effluent of the reactor, it proved to be essential to sustain a sufficiently high-pressure difference of the reactor outlet compared to the eluent stream. In combination with an automated valve sequence, the injection was furthermore highly reproducible and easy to operate during long-term investigations of the catalytic material.

Long-term stability of catalyst performance

The setup allows continuous operation of the microreactor and a large number of consecutive LC/MS analyses of the reactor effluent using a fully automated injection sequence. This enables long-term monitoring of catalyst performance, revealing the steady-state and potential deactivation of the catalyst.

As a first application, one chip-device reactor column was packed with Ley-Arvidsson-Yamamoto catalyst immobilized on silica (5 μm, 60 Å) to investigate a Mannich-reaction in μ-flow (Scheme 1B).

The reaction mixture was pumped through the reactor with a flow rate of 0.1 μL min^{-1}, resulting in a residence time of 90 s. In addition, benzanilide was added as an internal standard to counteract possible variations in the nanospray and pump performance. Thus, each HPLC/MS-measurement was normalized to the respective peak intensity and retention time of benzanilide, resulting in a highly reproducible chromatographic data acquisition (Figure 3B). The optimized on-chip separation revealed four different peaks of the *m/z*-ratio of the reaction product at four different retention times (t_R) of the HPLC-separation ($t_R = 6$, 8, 10, 11 min) referring to the *syn-* and *anti-*products and their respective (*S*)- and (*R*)-enantiomers. For further peak assignment, the reaction was conducted in batch with (*S*)- as well as with (*R*)-proline as catalytic species (11 h reaction time, 10 mol% proline each; shown in Figure S11 in the SI) and subsequently analyzed. According to previous results and the literature, it can be assumed that the first product peak ($t_R = 6$ min) refers to the *syn-*product **3**.[53,56]

ChemCatChem

Full Papers
doi.org/10.1002/cctc.202101148

Chemistry Europe
European Chemical
Societies Publishing

Scheme 1. A) Organocatalysts immobilized on silica packed in the respective reactor channel. B) Mannich reaction using hydrocinnamaldehyde as a substrate and an immobilized Ley-Arvidsson-Yamamoto catalyst; C) α-amination using an immobilized Jørgensen-Hayashi catalyst.

In order to investigate the long-term performance of the immobilized catalyst, a continuous-flow experiment was evaluated over 3 days on-stream (automized injections every 25 min, as shown in Figure 3C). The evaluation and normalization of the acquired data was facilitated by a tailored python script for an increased amount of acquisition data.

During the whole investigation, the immobilized catalyst proved to be highly enantio- and diastereoselective under the applied conditions, showing excellent er and dr with values higher than 95%. In total, the catalyst shows stable steady-state activity and maintains the very high stereoselectivity and enantioselectivity, now easily monitored over an extended time range with the presented method. For this quantity of valuable data, only microgram amounts of the catalytic material were necessary. Considering that three high-pressure pumps were used simultaneously for operating the fluidic setup and the integrated separation column, relatively low solvent consumption can be observed. Contemplating a flow rate of 75 μL min^{-1} for the elution flow along the separation column, total consumption of slightly more than a hundred milliliters of solvent for an 24 h operation is required. The additional consumption of the reactor and pinch flow rate is negligible in the range of less than 6 mL.

Catalyst optimization

In our previous publication,[53] an α-amination of aliphatic aldehydes over a TMS-protected Jørgensen-Hayashi catalyst on silica as support did not show the desired enantioselectivity towards the *S*-product as presented in the literature.[57] Only a racemic mixture was observed via this formerly presented micro-batch mode. Using the method as presented in this publication for the first time, the reaction was performed again with the TMS-protected catalyst while running under truly continuous-flow conditions. For this application, the reactor
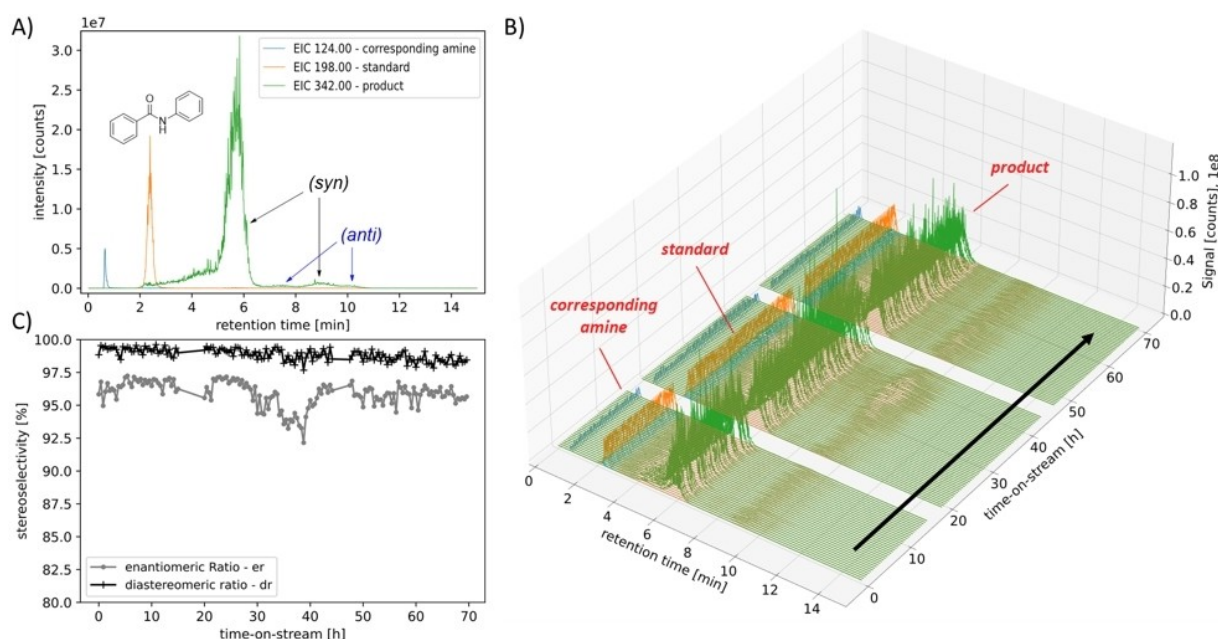

Figure 3. Long-term evaluation of catalyst performance for the Mannich reaction; A) Visualization of the LC-MS separation – showing the EICs of the amine (corresponding signal after hydrolysis of the starting material **2**), the respective stereoisomers of the reaction product and benzanilide as internal standard; B) long-term evaluation of the catalytic performance for approx. 3 days. with repetitive injections each 25 min. For daily maintenance of the system the data acquisition was stopped during two times, whereby the sample flow over the continuous reactor was still operated (after approx. 18 and 45 h). C) Course of the stereoselectivity of the catalyst, showing the enantiomeric (er) and diastereomeric ratio (dr).

ChemCatChem

Full Papers
doi.org/10.1002/cctc.202101148

Chemistry
Europe
European Chemical
Societies Publishing

was operated with a considerably low residence time of only 9 s (using a flow rate of 1 µl min⁻¹). Since the focus was on the enantioselectivity of the catalytic reaction, chiral HPLC/MS analysis was performed. From Figure 4A, the progression of the enantiomeric excess can be observed over the reactor's entire time-on-stream using on-line chiral HPLC/MS. In order to assign the respective peaks to the (S)- and (R)-enantiomer, the specific rotation value of the isolated product was measured and compared with literature data (as shown in the SI). The trends of the enantioselectivity in relation to the reactor's time-on-stream are shown in Figure 4B. The resulting data not only confirmed the poor selectivity of the TMS-protected catalyst (racemic mixture after 30 min), but also showed a slight trend towards the opposite R-enantiomer (ee of 25% (R) at 200 min runtime). As a lability of trimethyl-silyl ethers towards hydrolysis is well known from the literature,[58,59] other protecting groups were already applied.[60,57]

Since in our previous publication, such a strong deactivation process was not observed when using a polymer monolith as support,[61] we assume that by using silica, additional interactions between silanol groups on the support's surface and the catalyst could occur, which would amplify the deprotection by hydrolysis.

To prevent this desilylation process, a *tert*-butyldimethylsilyl group was used as a sterically more demanding and thus more stable protecting group in the next run. The results show a much-improved enantioselectivity of 74% (S) in the steady-state (at about 215 min runtime). To complete this investigation of the protecting group's influence on the enantioselectivity, we immobilized an unprotected version of the catalyst and studied the outcome of the amination reaction. Only minor amounts of the resulting product were observed as shown by the ratio of the product and reactant signals as shown in Figure 4C. The TBS-protected catalyst had a significantly higher product-to-reactant ratio than the TMS-protected variant (Figure 4C), despite a difference in loading numbers, which were in favor of the **TMS-JH** (0.38 mmol g⁻¹ for **TBS-JH** and 0.48 mmol g⁻¹ for **TMS-JH**). To our surprise, for the unprotected catalyst the enantioselectivity seemed to start favoring of the S-product (ee of 36% (S) after 12 min) and then slightly changed until a racemic mixture was observed in the catalyst's steady-state. This result is quite intriguing, and further studies would be necessary for a detailed mechanistic rationalization. Nevertheless, the outstanding advantage of the newly presented integrated chip system is the possibility to visualize such a dynamic course of changing stereochemistry while maintaining the continuous flow. As a first proof, the long-term performance of an asymmetric Mannich reaction was investigated using an immobilized Ley-Arvidsson-Yamamoto catalyst. Subsequently, we applied the setup to study the protecting group's influence of a Jørgensen-Hayashi catalyst in the α-amination of hydrocinnamaldehyde over the entire time-on-stream. With this first realization of such a continuous process control at a microscale, we look forward confidently to future work where additional functionalities could be integrated into one chip device to increase throughput and information gain.
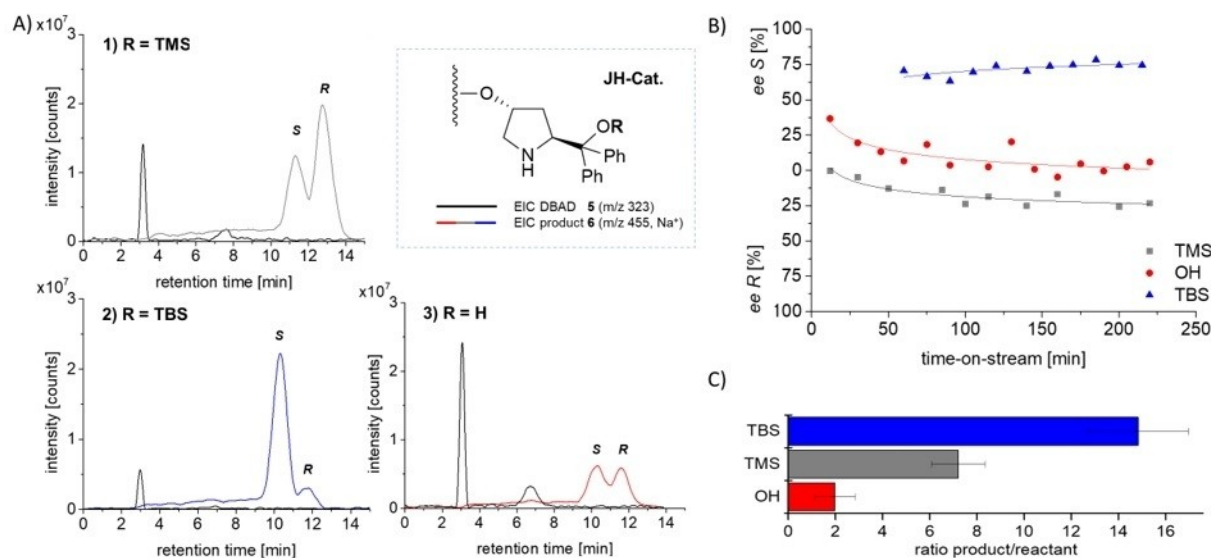

Figure 4. Comparison of the enantioselectivity of the α-amination using differently protected Jørgensen-Hayashi-catalysts immobilized on silica particles. A) 1) TMS-protection group at reactor runtime 220 min; 2) TBS protection group at reactor runtime 200 min; 3) no protection group at reactor runtime 205 min; Reactor flow: 1 µL min⁻¹, MeCN. Separation: Chiralpak IG-3, 3 µm. 75 µL min⁻¹, H₂O:MeCN (55:45 vol.%) with 0.1% FA, with a linear flow velocity of 1.6 mm s⁻¹ across the column. Pinch flow: 2 µL min⁻¹, H₂O:MeCN (50:50 vol.%) with 0.1% FA. Injection time: 10 sec; 10-point Savitzky-Golay smoothing; B) Trends of the ee as a function of the reactor time and the utilized protection group on the immobilized catalyst; C) Ratio of the product to the DBAD **5** signal using the respective areas averaged over the entire run.

ChemCatChem

Full Papers
doi.org/10.1002/cctc.202101148

Chemistry Europe
European Chemical
Societies Publishing

Conclusion

In this contribution, a new method for the analysis of continuous microflow processes of heterogeneous catalysis was presented using one single chip device as a centerpiece. With the described process control, minimal amounts of reactor effluent can be sampled and analyzed by the chip's chiral HPLC/MS unit without disturbing the steady-state operation of the flow reaction. For the first time, important observations of the catalysts' dynamic course of steady-state, stereoselectivity, and overall long-term activity can be made by using such miniature amounts of valuable catalyst materials. By gaining insights into the catalytic operation's steady-state, this method could be beneficial for potential upscaling at a later stage. Furthermore, this chip design can reduce the consumption of organic solvents for the analysis significantly, thus improving the method's overall environmental impact.

Experimental Section

Chip Layout and preparatory steps

The full glass chips were manufactured by an in-house protocol, including photolithography, wet etching, and high-temperature bonding. The protocol is described in detail in the SI. Briefly, the chip design consists of a 6 cm long separation channel (50–60 μm width) and a microreactor with a length of 9.5 cm (100 μm width), resulting in an estimated reactor volume of approximately 150 nl in its packed state (assuming an exclusion volume of 50%). Both channels are connected to a packing channel, sealed with photo-polymerized plugs after the respective material was introduced. The design includes constrictions (25 μm) at each end of the

column channel for the integration of photo-polymerized frits as particle-retaining elements. In order to realize a continuous discharge of the reactor effluent during continuous flow operation, an additional bypass channel is located at the end of the reactor. Subsequently, an injection cross is integrated to enable an almost dead-volume free sampling of the reactor effluent onto the separation column. For the detection via mass spectrometry, a pyramidal monolithic nano-spray emitter is grinded after the separation column. If necessary, an additional sheath channel can be used before the emitter to enable stabilization of the electro-spray by the addition of an aqueous fraction after the separation column.

Fluidic Setup

In the following section, the fluidic setup, as well as all connections and components of the instrumental setup as shown in Figure 5 are described in a detailed manner. For the construction of the fluidic circuit, four 10-port nanovolume valves (Cheminert, VICI AG, Schenkon, Switzerland) were used, whereby all fluidic connections were realized by commercially available PEEK capillary tubings (360 μm OD, 100 μm ID, VICI AG) and high-pressure PEEK fittings.

For increased stability and accessibility of the valves and the chip mounting, the setup was built on a metal stage with an integrated interface for MS-coupling. On this metal platform, an xyz-linear translation stage (T12XYZ, Thorlabs GmbH, Dachau, Germany) was utilized to mount and align the monolithic chip emitter in front of the MS. The connections of the chips to the capillaries and valves were realized by a high-pressure steel clamp system enabling direct fluidic contact with minimized dead volume.[62] To facilitate a semi-automated injection sequence, the valves were connected to electric actuators and a Chromatography Data Station (Clarity, DataApex, Prague, Czech Republic).

For monitoring the performance of the system, flow and pressure sensors were integrated. The flow along the reactor column was
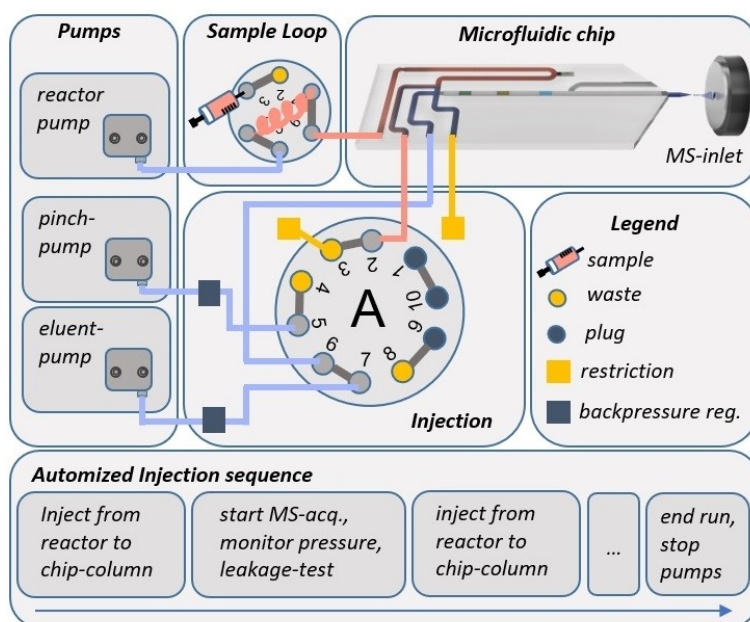

Figure 5. Schematic overview of the instrumental fluidic setup, including valves and the duty cycle of the automated injection sequence.

ChemCatChem

Full Papers
doi.org/10.1002/cctc.202101148

**Chemistry
Europe**
European Chemical
Societies Publishing

realized by using an LC-20AD HPLC pump (Shimadzu, Kyoto, Japan). A modulated 1260 Infinity HPLC system with a binary and isocratic pump (Agilent, Santa Clara, USA) was used for the elution flow along the separation column. To increase the stability of the eluent flow, additional active backpressure regulators (BPR2, VICI AG) were added after the pumps, as well as restriction capillaries after the chip outlet to increase the split ratio towards the separation column and thus reduce the eluent consumption to a minimum. In-line filters were placed after the pumps and inlets, as well as after the bypass outlet connection from the chip to avoid any contamination by particles.

Catalyst synthesis and immobilization

The immobilized Ley-Arvidsson-Yamamoto catalyst was synthesized by thermal/photoinduced thiolene coupling, starting from mercaptopropyl silica gel (5 μm, 60 Å, Sigma Aldrich), as described in a previous publication.[56]

For the α-amination reaction, Jørgensen-Hayashi catalysts with different protecting groups were synthesized and subsequently immobilized onto commercial porous silica particles (Kromasil, 5 μm, Nyouron) via copper(I)-catalyzed alkyne-azide cycloaddition. A detailed description of the synthetic method can be found in the supplementary information (SI).

Continuous flow catalysis

For the Mannich reaction, the reaction mixture consisted of 9.6 mM hydrocinnamaldehyde **1** and 1.0 mM N-PMP-ethyl-iminoglyoxylate **2** in MeCN (Scheme 1A). For the α-amination, the reaction mixture consisted of 1.25 mM **4**, 6.25 mM dibenzyl azodicarboxylate **5**, and 0.625 mM CH$_3$COOH in MeCN (Scheme 1B).

The packed bed microreactor contained less than 200 μg of the respective catalytic material. The reactions were carried out at room temperature with a flow rate of 0.1 μL min^{-1} (Mannich reaction) and 1 μL min^{-1} (α-amination) through the microreactor unit of the chip (90 s and 9 s residence time, respectively).

Conflict of Interest

The authors declare no conflict of interest.

[1] M. Colella, C. Carlucci, R. Luisi, *Top. Curr. Chem.* **2018**, *376*, 46.
[2] F. Fanelli, G. Parisi, L. Degennaro, R. Luisi, *Beilstein J. Org. Chem.* **2017**, *13*, 520–542.
[3] Y. Liu, X. Jiang, *Lab Chip* **2017**, *17*, 23, 3960–3978.
[4] C. Rodríguez-Escrich, M. A. Pericàs, *Chem. Rec.* **2019**, *19*, 1872–1890.
[5] J. Yoshida, Y. Takahashi, A. Nagaki, *Chem. Commun.* **2013**, *49*, 9896–9904.
[6] I. R. Baxendale, *J. Chem. Technol. Biotechnol.* **2013**, *88*, 519–552.
[7] B. Gutmann, D. Cantillo, C. O. Kappe, *Angew. Chem. Int. Ed.* **2015**, *54*, 6688–6728; *Angew. Chem.* **2015**, *127*, 6788–6832.
[8] M. B. Plutschack, B. Pieber, K. Gilmore, P. H. Seeberger, *Chem. Rev.* **2017**,*117*, 18, 11796–11893.
[9] F. Ferlin, D. Lanari, L. Vaccaro, *Green Chem.* **2020**, *22*, 5937–5955.
[10] M. Guidi, P. H. Seeberger, K. Gilmore, *Chem. Soc. Rev.* **2020**, *49*, 8910–8932.
[11] C. D. Risi, O. Bortolini, A. Brandolese, G. D. Carmine, D. Ragno, A. Massi, *React. Chem. Eng.* **2020**, *5*, 1017–1052.
[12] D. Dallinger, C. O. Kappe, *Curr. Opin. Green Sustain. Chem.* **2017**, *7*, 6–12.
[13] D. Zhao, K. Ding, *ACS Catal.* **2013**, *3*, 928–944.
[14] V. Hessel, *Chem. Eng. Technol.* **2009**, *32*, 1655–1681.
[15] K. Geyer, J. D. C. Codée, P. H. Seeberger, *Chem. Eur. J.* **2006**, *12*, 8434–8442.
[16] K. Geyer, T. Gustafsson, P. H. Seeberger, *Synlett* **2009**, 2382–2391.
[17] J. P. McMullen, K. F. Jensen, *Annu. Rev. Anal. Chem.* **2010**, *3*, 19–42.
[18] S. V. Ley, D. E. Fitzpatrick, R. J. Ingham, R. M. Myers, *Angew. Chem. Int. Ed.* **2015**, *54*, 3449–3464; *Angew. Chem.* **2015**, *127*, 3514–3530.
[19] A.-C. Bédard, A. Adamo, K. C. Aroh, M. G. Russell, A. A. Bedermann, J. Torosian, B. Yue, K. F. Jensen, T. F. Jamison, *Science* **2018**, *361*, 1220–1225.
[20] M. Trojanowicz, *Molecules* **2020**, *25*, 1434.
[21] T. Yu, Z. Ding, W. Nie, J. Jiao, H. Zhang, Q. Zhang, C. Xue, X. Duan, Y. M. A. Yamada, P. Li, *Chem. Eur. J.* **2020**, *26*, 5729–5747.
[22] S. Kobayashi, *Chem. Asian J.* **2016**, *11*, 425–436.
[23] R. Porta, M. Benaglia, A. Puglisi, *Org. Process Res. Dev.* **2016**, *20*, 2–25.
[24] B. Martin, H. Lehmann, H. Yang, L. Chen, X. Tian, J. Polenk, B. Schenkel, *Curr. Opin. Green Sustain. Chem.* **2018**, *11*, 27–33.
[25] V. R. L. J. Bloemendal, M. A. C. H. Janssen, J. C. M. van Hest, F. P. J. T. Rutjes, *React. Chem. Eng.* **2020**, *5*, 1186–1197.
[26] D. L. Hughes, *Org. Process Res. Dev.* **2020**, *24*, 1850–1860.
[27] S. B. Ötvös, C. O. Kappe, *Green Chem.* **2021**, *23*, 6117–6138 .
[28] D. Perera, J. W. Tucker, S. Brahmbhatt, C. J. Helal, A. Chong, W. Farrell, P. Richardson, N. W. Sach, *Science* **2018**, *359*, 429–434.
[29] J. A. Bennett, Z. S. Campbell, M. Abolhasani, *Curr. Opin. Chem. Eng.* **2019**, *26*, 9–19.
[30] M. Berton, J. M. de Souza, I. Abdiaj, D. T. McQuade, D. R. Snead, *J. Flow Chem.* **2020**, *10*, 73–92.
[31] L. Rogers, N. Briggs, R. Achermann, A. Adamo, M. Azad, D. Brancazio, G. Capellades, G. Hammersmith, T. Hart, J. Imbrogno, L. P. Kelly, G. Liang, C. Neurohr, K. Rapp, M. G. Russell, C. Salz, D. A. Thomas, L. Weimann, T. F. Jamison, A. S. Myerson, K. F. Jensen, *Org. Process Res. Dev.* **2020**, *24*, 2183–2196.
[32] A. J. deMello, *Nature* **2006**, *442*, 394–402.
[33] D. C. Fabry, E. Sugiono, M. Rueping, *React. Chem. Eng.* **2016**, *1*, 129–133.
[34] K. F. Jensen, *AIChE J.* **2017**, *63*, 858–869.
[35] R. A. Potyrailo, R. J. Wroczynski, J. P. Lemmon, W. P. Flanagan, O. P. Siclovan, *J. Comb. Chem.* **2003**, *5*, 8–17.
[36] R. Herzig-Marx, K. T. Queeney, R. J. Jackman, M. A. Schmidt, K. F. Jensen, *Anal. Chem.* **2004**, *76*, 6476–6483.
[37] S.-A. Leung, R. F. Winkle, R. C. R. Wootton, A. J. deMello, *Analyst* **2005**, *130*, 46–51.
[38] J. Yue, J. C. Schouten, T. A. Nijhuis, *Ind. Eng. Chem. Res.* **2012**, *51*, 14583–14609.
[39] P. Beato, E. Schachtl, K. Barbera, F. Bonino, S. Bordiga, *Catal. Today* **2013**, *205*, 128–133.
[40] V. Sans, L. Porwol, V. Dragone, L. Cronin, *Chem. Sci.* **2015**, *6*, 1258–1264.
[41] B. A. Rizkin, F. G. Popovic, R. L. Hartman, *J. Vac. Sci. Technol. A* **2019**, *37*, 5, 050801.
[42] S. Chatterjee, M. Guidi, P. H. Seeberger, K. Gilmore, *Nature* **2020**, *579*, 379–384.
[43] N. Holmes, G. R. Akien, R. J. D. Savage, C. Stanetty, I. R. Baxendale, A. J. Blacker, B. A. Taylor, R. L. Woodward, R. E. Meadows, R. A. Bourne, *React. Chem. Eng.* **2016**, *1*, 96–100.
[44] A. Echtermeyer, Y. Amar, J. Zakrzewski, A. Lapkin, *Beilstein J. Org. Chem.* **2017**, *13*, 150–163.
[45] J. P. McMullen, K. F. Jensen, *Org. Process Res. Dev.* **2011**, *15*, 398–407.
[46] B. J. Reizman, K. F. Jensen, *Org. Process Res. Dev.* **2012**, *16*, 1770–1782.
[47] N. Holmes, G. R. Akien, A. J. Blacker, R. L. Woodward, R. E. Meadows, R. A. Bourne, *React. Chem. Eng.* **2016**, *1*, 366–371.

[48] E. S. Isbrandt, R. J. Sullivan, S. G. Newman, *Angew. Chem. Int. Ed.* **2019**, *58*, 7180–7191; *Angew. Chem.* **2019**, *131*, 7254–7267.

[49] D. Krištofíková, V. Modrocká, M. Mečiarová, R. Šebesta, *ChemSusChem* **2020**, *13*, 2828–2858.

[50] I. Atodiresei, C. Vila, M. Rueping, *ACS Catal.* **2015**, *5*, 1972–1985.

[51] C. Lotter, E. Poehler, J. J. Heiland, L. Mauritz, D. Belder, *Lab Chip* **2016**, *16*, 4648–4652.

[52] J. J. Heiland, R. Warias, C. Lotter, L. Mauritz, P. J. W. Fuchs, S. Ohla, K. Zeitler, D. Belder, *Lab Chip* **2017**, *17*, 76–81.

[53] R. Warias, A. Zaghi, J. J. Heiland, S. K. Piendl, K. Gilmore, P. H. Seeberger, A. Massi, D. Belder, *ChemCatChem* **2018**, *10*, 5382–5385.

[54] R. H. Crabtree, *Chem. Rev.* **2015**, *115*, 127–150.

[55] C. Hammond, *Green Chem.* **2017**, *19*, 2711–2728.

[56] O. Bortolini, L. Caciolli, A. Cavazzini, V. Costa, R. Greco, A. Massi, L. Pasti, *Green Chem.* **2012**, *14*, 992.

[57] X. Fan, S. Sayalero, M. A. Pericàs, *Adv. Synth. Catal.* **2012**, *354*, 2971–2976.

[58] T. D. Nelson, R. D. Crouch, *Synthesis* **1996**, *1996*, 1031–1069.

[59] E. Alza, M. A. Pericàs, *Adv. Synth. Catal.* **2009**, *351*, 3051–3056.

[60] I. Mager, K. Zeitler, *Org. Lett.* **2010**, *12*, 7, 1480–1483.

[61] R. Warias, D. Ragno, A. Massi, D. Belder, *Chem. Eur. J.* **2020**, *26*, 13152–13156.

[62] C. Lotter, J. J. Heiland, V. Stein, M. Klimkait, M. Queisser, D. Belder, *Anal. Chem.* **2016**, *88*, 7481–7486.